MEASUREMENT OF THE SPECIFIC HEAT CAPACITY OF COPPER NANOFLUIDS BY MODULATED TEMPERATURE DIFFERENTIAL SCANNING CALORIMETRY

Eveline De Robertis, erobertis@inmetro.gov.br
Priscila Laviola Sanches, priscilalavi@hotmail.com
Rodrigo de Santis Neves, rsneves@inmetro.gov.br
Alexei Yu. Kuznetsov, okuznetsov@inmetro.gov.br
Andrea Porto Carreiro Campos, apcampos@inmetro.gov.br
Sandra Marcela Landi, smlandi@inmetro.gov.br
Divisão de Metrologia de Materiais, INMETRO, Duque de Caxias - RJ, Brasil

Carlos Alberto Achete, achete@metalmat.ufrj.br
Divisão de Metrologia de Materiais, INMETRO, Duque de Caxias - RJ, Brasil
COPPE - Programa de Engenharia Metalúrgica e de Materiais, UFRJ, Rio de Janeiro - RJ, Brasil

Abstract. *The purpose of this study is to apply the Modulated Temperature Differential Scanning Calorimetry technique to measure the specific heat capacity of copper nanofluids by using the method described in the standard ASTM E2716-09, which is generally applied to termally stable solids and liquids. This technique was applied in nanofluids prepared by one-step method, using sodium hypophosphite as reducing agent in ethylene glycol base fluid. Polyvinyl pyrrolidone (PVP) was used as stabilizing agent for copper particles obtained from two different precusor salts, copper nitrate and copper sulphate. The particles were examined by X-Ray Diffraction (XRD) and Transmission Electron Microscopy (TEM) in order to evaluate their structure, shape, size and chemical nature. The presence of copper nanoparticles in the base fluid alters its characteristics of crystalization and melting and reduces the specific heat capacity values by c.a. 220-275 mJ* g^{-1} K^{-1}.

Keywords*: copper nanofluid, specific heat capacity, Modulated Temperature Differential Scanning Calorimetry*

1. INTRODUCTION

The research in heat transfer field has received a great boost and a renewed interest in recent years because of the increasing demand of cooling systems with more efficient heat exchange capacity. Two main approaches to increase the cooling efficiency can be pointed out: the introduction of new geometries in cooling systems and the increase of the heat exchange capacity of the fluids used in thermal systems. In many cases, however, the design restrictions make impossible to use the geometrical factor to increase the heat removal from the system. In contrast, the heat exchange properties of a refrigerant can be considerably improved without affecting the geometry of the whole system by introducing in the fluid medium particles with high thermal conductivity. In the past, this approach was tested using refrigerants with particles of micrometric size or bigger. This led to unsatisfactory results due to the various phenomena encountered in such fluids: rapid sedimentation of suspensions, erosion of heat exchange devices and products, obstruction of pipes, high-pressure loss, etc. Recent results showed, however, that the addition of nanometric size particles in refrigerants can increase considerably the thermal conductivity of fluids, with maintained stability (Yu *et al.* 2008).

The specific heat capacity and the thermal conductivity of these kinds of suspensions are two among the most important thermal properties that affect the heat transfer process. Therefore, for dealing with controllable flow and heat transfer processes, it is necessary to understand the mechanism involving such parameters (Xuan *et al.* 2009). Only several papers reported data of the specific heat capacities of nanofluids in different systems obtained with different techniques, for example: Zhou and Ni (2008) studied water-based Al_2O_3 nanofluid and Xuan *et al.* (2009) studied magnetic microencapsulated suspension, both employed a power compensated differential scanning calorimeter and Zhou *et al.* (2010) studied CuO/Etylene glycol system using an apparatus designed for measurements employing the quasi-steady-state method.

Differential scanning calorimetry (DSC) is a thermal analysis technique used for more than thirty years to measure a wide variety of material properties including heat capacity. Although most DSC measurements are simple, fast and accurate, and require only a single experiment, the measurement of heat capacity usually requires a minimum of three experiments and provided accuracies typically good to only ±10% (ASTM E1269-05).

Modulated temperature differential scanning calorimetry (MTDSC) is a new technique, introduced in 1992, which provides not only the same information as conventional DSC, but also information not available from conventional DSC by overcoming most of the limitations, such as: the ability to properly analyze complex transitions, the presence of sufficient sensitivity, the presence of adequate resolution and the need of complex experiments.

MTDSC differs from conventional DSC in that a low-frequency sinusoidal or non-sinusoidal perturbation ranging from approximately 0.001 to 0.1 Hz (1000-10 s period) is overlaid on the baseline temperature profile. The use of a complex temperature modulation allows the response to multiple frequencies to be measured at one time.

The most common MTDSC data analysis involves separating the total heat flow or apparent heat capacity into reversing and non-reversing components. The reversing component of the heat flow is obtained from the amplitude of the first harmonic of the heat flow A_{mhf}, using a Fourier transform of the data (or an approximation). Dividing by the amplitude of the applied heating rate, A_{mrh}, gives the reversing component of the apparent heat capacity:

$$C_{p,rev} = \frac{A_{mhf}}{W_s A_{mrh}} \tag{1}$$

where W_s is the mass of the sample. The heat flow amplitude can be measured directly in a power-compensated DSC and can be calculated from the temperature difference between the sample and the reference in a heat flux DSC. The applied temperature profile is known which allows the calculation of heating rate assuming that the sample is able to follow the applied temperature profile. For example, for a sinusoidal temperature profile:

$$T = T_0 + \beta t + A_{mhr} \sin(\omega t) \tag{2}$$

$$A_{mhr} = \omega A_{\dot{mhr}} \tag{3}$$

where β is the heating rate, and $A_{\dot{mhr}}$ and ω are the amplitude and frequency of the perturbation, respectively. T and T_0 are the temperatures of the sample at time t and at time t=0 when the sample follows the applied furnace temperature. The non-reversing heat flow is defined as the difference between the average heat flow $\langle P \rangle$ and the reversing heat flow; the non-reversing heat capacity is the difference between the normalized average heat flow divided by the underlying heating rate β and the reversing heat capacity:

$$C_{p,non} = \frac{\langle P \rangle}{W_s \beta} - C_{p,rev} \tag{4}$$

In the absence of thermal events, the reversing heat capacity is simply the frequency-independent heat capacity C_p and the non-reversing heat capacity is zero, otherwise, the reversing heat flow was initially considered to only reflect reversible sensible heat effects due to changes in the heat capacity, whilst the non-reversing heat flow was considered to reflect primarily irreversible kinetic effects. The assumption that the sensible heat and kinetics effects can be equated to reversing and non-reversing heat capacities (or heat flows) is valid only if the kinetics associated with the processes being measured are linear and if the kinetic response does not have contributions to the first harmonic (Simon 2001).

As one of the advantages of MTDSC is the ability to measure the absolute heat capacity without the need to make multiple runs, this study was performed in order to understand if nanofluids heat capacity measurements can be realized by this technique instead employing conventional DSC measurements.

2. EXPERIMENTAL

The nanofluids were prepared directly in the base fluid. This method consists in metallic nanoparticles synthesis from inorganic salts precursors, primarily dissolved in the base fluid and subsequently reduced to form metallic nanoparticles through chemical reaction with reducing species in the presence of stabilizing agents. The stabilizing agents are organic molecules with long linear carbon chains, preferably, that adsorb on the first nuclei surface of the metallic nanoparticles, stabilizing them and therefore suppressing the growth process and favoring the nucleation of other colloidal particles

Ethylene glycol was used as base fluid, two different inorganic salts were used to prepare the nanofluids, copper nitrate and copper sulphate, sodium hypophosphite was used as reducing agent and polyvinyl pyrrolidone (PVP) was used as stabilizer. The nanofluids were synthesized using a microwave reactor in pulse mode, without further dispersion.

DSC and MTDSC measurements were carried out on a DSC Q2000 from TA Instruments in T0 aluminum hermetic pans. The temperature and heat flow signals were calibrated in accordance with Practice E967 and E968, respectively, using an indium certified reference material from NIST. The heat capacity signal for specific heat capacity measurements under modulated temperature conditions was calibrated in accordance with Practice E2716, using

synthetic sapphire disc reference material and verified with a synthetic sapphire certified reference material from NIST, in cylindrical shape.

The samples were homogenized before being encapsulated and weighed after the experiment for determining the mass change and the validity of the measure. All runs were conducted under dynamic nitrogen atmosphere (50 mL/min). Two different cooling/heating rates (20 and 2 °C) and volumes (10 and 20 µL) were used in DSC experiments in order to examine the influence of these parameters in ethylene glycol thermal behavior. MTDSC runs were recorded using 3 °C/min cooling/heating rate, ± 1.0 °C amplitude, 100 s period (10 mHz frequency) and -60 to 100 °C temperature range.

The samples will be named as follows: pure ethylene glycol (EG); copper nanofluid obtained from copper nitrate (NFLN); copper nanofluid obtained from copper sulphate (NFLS); copper nanoparticle separated from NFLN (NPN); copper nanoparticle separated from NFLS (NPS).

The stability of the samples was followed observing the particles sedimentation over time in steady state in a graduated cylinder.

X-Ray powder diffraction patterns (XRD) were obtained with a D8-Focus diffractometer from Bruker using Cu Kα radiation with the step size of 0.02 ° and acquisition time of 30 s/step for NPN and 12 s/step for NPS. The calculations of particle mean size were made employing the Topas-Academic software (Coelho 2007). The particles were separated from the fluid by centrifugation, then washed with ethanol and centrifuged for several times and dried under nitrogen flux.

Morphology studies of copper particles were carried out by Transmission Electron Microscopy (TEM). TEM images were obtained in C_s probe corrected Titan 80-300 kV from FEI company operating at 300 kV. The samples were prepared from 10 µL aliquots of the nanofluids dissolved in 1 mL of ethanol and sonicated. 5 µL aliquots were dripped in copper grid and dried under nitrogen flux.

3. RESULTS AND DISCUSSION

3.1. Nanoparticles characterization

Figure 1A shows XRD patterns of nanoparticles separated from their respective nanofluids as described in the previous section. Two chemical species can be identified from these patterns: metallic copper (Cu) and copper (I) oxide (cuprous oxide Cu_2O), whose theoretical main diffraction lines are presented in Fig. 1B and can be related to experimental XRD patterns.

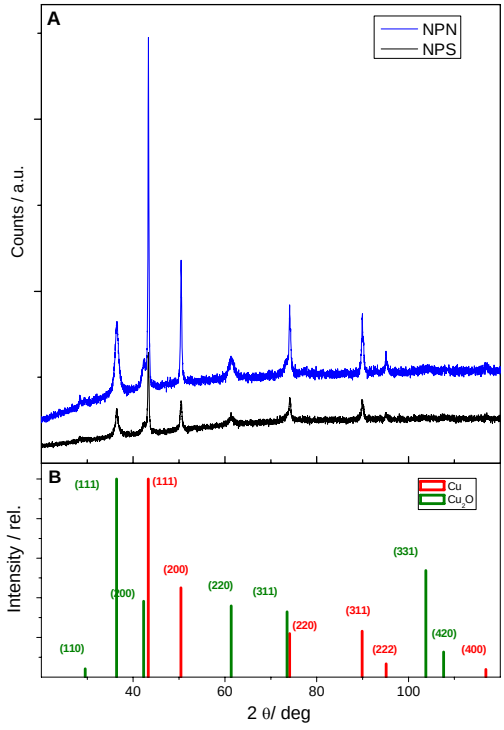

Figure 1. Experimental XRD pattern of nanoparticles from nanofluids NFLN and NFLS (A). Main diffraction lines of Cu and Cu_2O (B)

Besides the attempts to preserve the natural state of the particles after they have been removed from the fluid, some of them might have been oxidized by atmospheric oxygen, therefore is difficult to attribute the presence of both species in the nanofluid. The particles mean sizes obtained from calculations based on the diffraction patterns are 29.69 nm and 67.67 nm for NFLN and NFLS, respectively.

The selected micrographs presented in Fig. 2 revealed some interesting aspects. The presence of phosphorus was observed in EDS analysis (Fig. 2A), it can be attributed to some phosphorus from reducing agent present in nanofluid and not completely washed during sample preparation, since no alloys of copper with phosphorus were identified by XRD. It can be seen from fig. 2B that several agglomerates were formed after NFLS preparation, where particles from 50 to almost 2000 nm can be observed and this characteristic was reflected by the instability of this fluid. In NFLS all particles sedimented in four days while the sedimentation rate of NFLN was c.a. 10% in the two first weeks, increasing with the time due to larger particles drag the smaller particles to the bottom of the flask in the following two weeks, this can be related to a better particle distribution on PVP surface as can be seen in Fig. 2A. Also in Fig. 2A can be observed that the particles are smaller in NFLN than in NFLS. Despite the formation of several agglomerates, some particles with around 60 nm can be identified in Fig. 2B, confirming the calculations of particles mean size from XRD patterns.

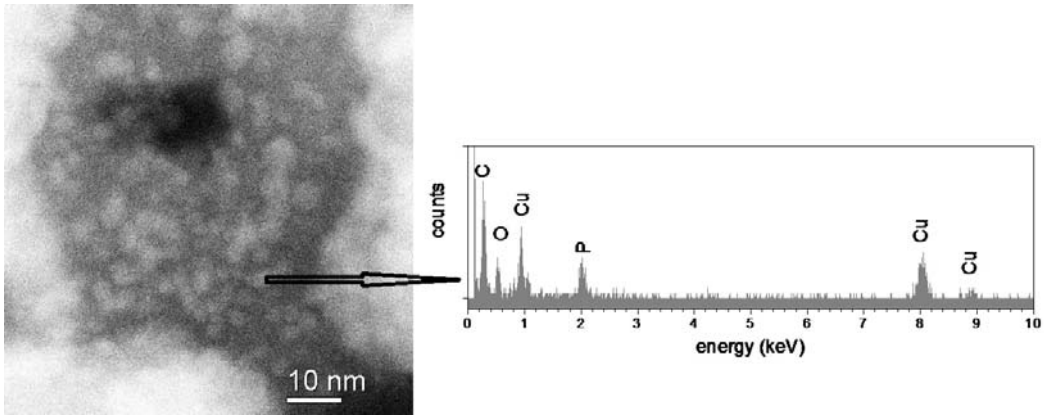

A

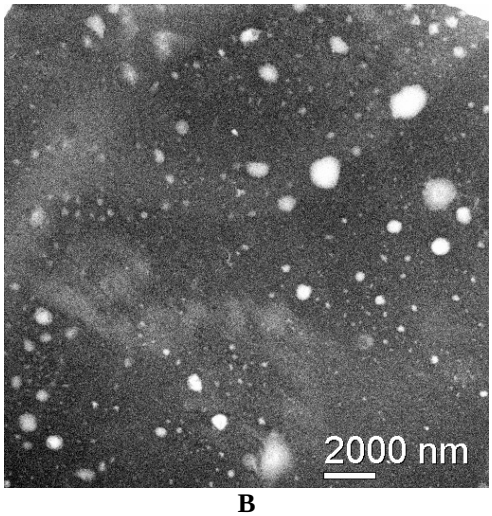

B

Figure 2. Selected TEM micrographs of nanoparticles from nanofluids: NFLN and EDS pattern (A) and NFLS (B)

3.2. DSC experiments

The influence of cooling/heating rate for EG samples were studied in order to identify the processes of crystallization and melting, however no peaks of such transitions were identified in both the used scan rates (Fig. 3A). This fact points to the formation of an amorphous solid phase. The increase of volume (Fig. 3B) did not change the freezing EG characteristics, however some small differences in heat flow can be observed above 0 °C during the heating.

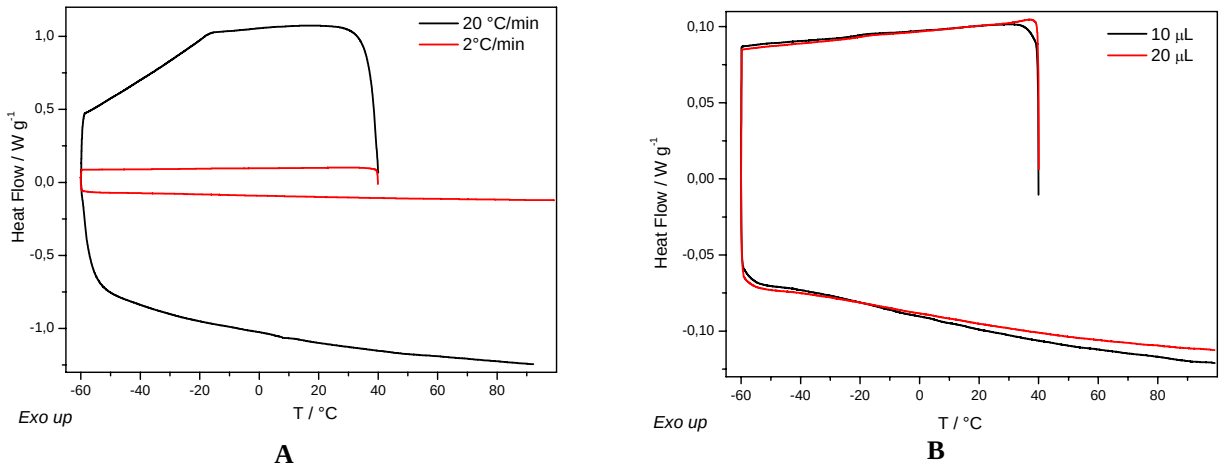

Figure 3. Heat flow curves of EG under dynamic atmosphere of N_2 (50 mL/min) obtained at different heating/cooling rates (A) and different volumes at 2 °C/min (B).

Figure 4 shows heat flow curves of nanofluids prepared for this study and their components: pure base fluid and nanoparticles separated from each other. These curves were taken with a qualitative purpose, mainly to observe the behavior related to nanoparticles presence in the base fluid. The first observation is that the nanoparticles in the fluid causes a small decrease in heat flow values in temperatures where no transitions are observed. The second observation is that the nanofluids crystallize in temperatures below -50 °C, in a very strong exothermic process. The crystallization process can be distinguished in nanofluids because the presence of nanoparticles generates nucleation points for crystal formation. The onset temperature related to the melting process are very close for both nanofluids and the minimum temperature peak of both nanofluids is very close to the melting temperature of ethylene glycol (-13 °C).

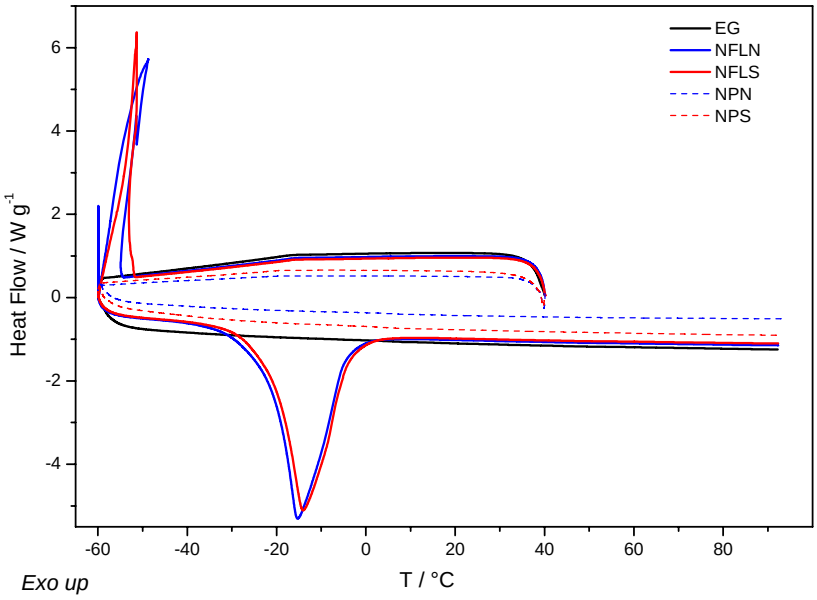

Figure 4. Heat flow curves of EG, NFLN, NFLS, NPN and NPS under dynamic atmosphere of N_2 (50 mL/min). Cooling /heating rate of 20 °C/min

3.3. MTDSC Experiments

To verify the validity of our heat capacity measurements using MTDSC, two samples of sapphire reference materials with different shapes were tested. Figure 5 shows specific heat capacity curves, calculated with the method described in the introduction section in accordance with Practice E2716. The smallest contact area of sapphire from NIST due to its cylindrical shape is responsible for the decrease in heat capacity values. The deviations obtained in this measurement compared with tabulated sapphire heat capacities (E1269) are 2.8 % and 5.9 % for disk and cylinder

sapphires, respectively. The sapphire heat capacities at 26.86 °C are 0.7792, 0.7574 and 7.329 J · g $^{-1}$ K^{-1} for tabulated, disk and cylinder, respectively.

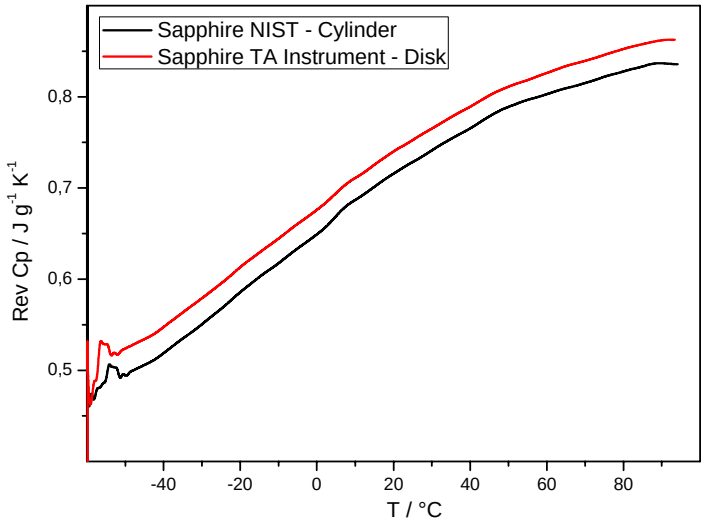

Figure 5. Specific heat capacity curves of Sapphires reference materials under dynamic atmosphere of N_2 (50 mL/min)

Figure 6 shows specific heat capacity curves of nanofluids prepared for this study and their components: pure base fluid and nanoparticles separated from each one. Table 1 contains the experimental values of heat capacities at 25 °C and 80 °C, as well as the values calculated from the data available in NIST webbook home pages for ethylene glycol, copper and cuprous oxide.

As EG sample did not present any transition as observed before in heat flow curve, the heat capacity curve is represented by a flat line with a small increase with the temperature (Fig 6). The observed peak in nanofluids heat capacity curves are related to the melting process.

In order to relate heat capacity measurements to thermal conductivity of the nanofluids, the improvement of the later will be indicated if a decrease in heat capacity values occurs. As can be seen more clearly in inset of Fig. 6, in the range of 0 °C to 90 °C, the lowest heat capacity values belong to the nanoparticles samples (NPN and NPS), and the highest to pure ethylene glycol (EG). The nanofluids heat capacity curves (NFLN and NFLS) lies between EG and nanoparticles curves. Therefore, there is some improvement in thermal conductivity of the fluid in presence of copper nanoparticles.

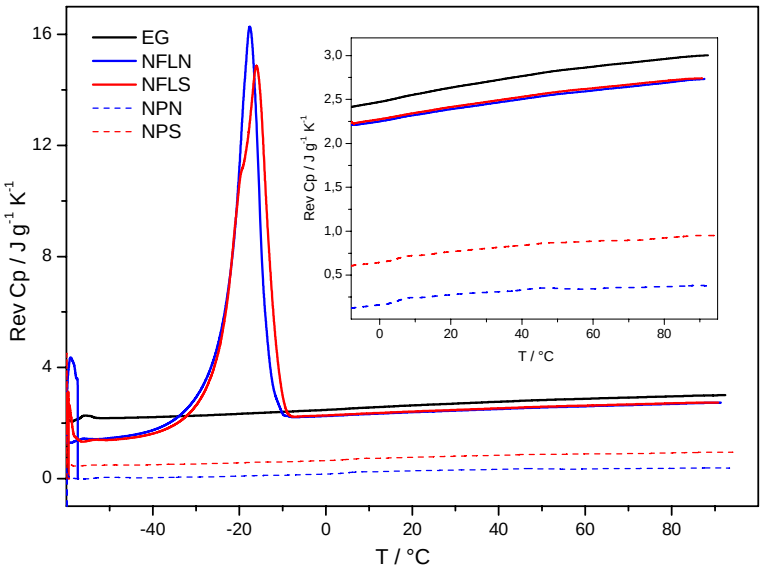

Figure 6. Specific heat capacity curves of EG, NFLN, NFLS, NPN and NPS under dynamic atmosphere of N_2 (50 mL/min)

The decrease in heat capacity obtained is in the range of 225 - 275 mJ · g $^{-1}$ K^{-1} in temperature range of 0 – 95 °C. This decrease in heat capacity represents an improvement of heat exchange ability in the order of 8 – 10 %.

Some remarks about the heat capacity observed for nanoparticles can be done. A decrease in heat capacity of nanoparticles is expected (Zhou *et al.* 2010) due to particle size when compared with calculated values for bulk samples showed in Table 1. However an increase in heat capacity is observed for NPS, this fact can be explained by the higher degree of particle agglomeration in NFLS, some PVP residual in the separated particles can contribute to the increase of NPS specific heat capacities observed in these experiments, since PVP heat capacity is expected to be higher than Cu or Cu_2O heat capacities.

Table 1. Selected experimental and calculated heat capacities of copper nanofluids and their separated components.

Sample	C_p **@ 25 °C / J · g $^{-1}$ K^{-1}**	C_p **@ 80 °C / J · g $^{-1}$ K^{-1}**
EG	2.6675	2.9598
NFLN	2.4173	2.688
NFLS	2.4425	2.7105
NPN	0.2924	0.3683
NPS	0.7856	0.9231
EG (1)	2.4135	-
Cu	0.3851	0.3971
Cu_2O	0.4370	0.4586

(1): calculated

4. CONCLUSIONS

In this work the importance of the method of preparation in order to obtain a long term stable nanofluid was showed, however, when the nanofluid freshly prepared is experimented, only small differences in the thermal behavior between both of them can be observed.

The application of the MTDSC for heat capacities determination presented good agreement between the tabulated values and experimental data for the standard reference materials. When applied to the studied nanofluidos, MTDSC also showed a good agreement between experimental heat capacities of the nanofluids separated components and tabulated values, showing that MTDSC is a valid technique for nanofluids heat capacities determination. Besides that, copper nanofluids prepared by one step technique showed an increase in the range of 8 – 10% in the nanofluids heat exchange ability based on heat capacity determinations.

5. ACKNOWLEDGEMENTS

The authors are grateful to the Brazilian agencies: Financiadora de Estudos e Projetos (FINEP), Fundação de Amparo à Pesquisa do Estado do Rio de Janeiro (FAPERJ) and Conselho Nacional de Desenvolvimento Científico e Tecnológico (CNPq).

6. REFERENCES

ASTM E1269-05, "Standard Test Method for Determining Specific Heat Capacity by Differential Scanning Calorimetry", ASTM International, 6 p.

ASTM E2716-09, "Standard Test Method for Determining Specific Heat Capacity by Sinusoidal Modulated Temperature Differential Scanning Calorimetry", ASTM International, 4 p.

Cheng, L., Bandarra Filho, E.P. and Thome, J.R., 2008, "Nanofluid Two-Phase Flow and Thermal Physics: A New Research Frontier of Nanotechnology and Its Chalenges", Vol. 8, No. 8, pp.1-18.

Coelho A., 2007, "TOPAS-Academic V4.1", <http://www.topas-academic.net>.

Schawe, J.E.K., 1997, "Principles for the Interpretation of Temperature-Modulated DSC Measurements. Part 2: A Thermodynamic Approach", Thermochimica Acta, Vol.v304/305, pp. 111-119.

Simon, S.L., 2001, "Temperature-Modulated Differential Scanning Calorimetry: Theory and Application", Thermochimica Acta, Vol. 374, pp. 55-71.

Zhou, L-P., Wang, B-X., Peng, X-F., Du, X-Z. and Yang, Y-P., 2010, "On the Specific Heat Capacity of CuO Nanofluid", Advances in Mechanical Engineering, Vol. 2010, 4 p.

Wang, L. and Fan, J., 2010, "Nanofluid Research: Key Issues", Nanoscale Research Letters, DOI: 10.1007/s11671-010-9638-6.

Wong, K.V. and De Leon, O., 2010, "Applications of Nanofluids: Current and Future", Advances in Mechanical Engineering, Vol. 2010, 11 p.

Xuan, Y., Huang, Y. and Li, Q., 2009, "Experimenta Investigation on Thermal Conductivity and Specific Heat Capacity of Magnetic Microencapsulated Phase Change Material Suspension", Chemical Physics Letters, Vol. 479, pp. 264-269.

Yu, W., Frace, D.M., Routbort, J.L. and Choi, S.U.S., 2008, "Review and Comparison of Nanofluid Thermal Conductivity and Heat Transfer Enhancements", Heat Transfer Engineering, Vol. 29, No. 5, pp. 432-460.

Zhang, J., Zheng, Y., Yang, X. and Wang, R., 2008, "The Synthesis of a Second Generation of Nanofluids Based on Carbon Nanotubes", Acta Polymerica Sinica, Vol. 12, pp. 1209-1213.

Zhou, S-Q. and Ni, R., 2008, "Measurement of the Specific Heat Capacity of Water-Based Al_2O_3 Nanofluid", Applied Physics Letters, Vol. 92, 093123.

NIST webbook homepages:
<http://webbook.nist.gov/cgi/cbook.cgi?ID=C107211&Units=SI&Mask=2#ref-10> (Ethylene glycol)
<http://webbook.nist.gov/cgi/cbook.cgi?ID=C1317391&Units=SI&Mask=2#Thermo-Condensed> (Cu2O)
<http://webbook.nist.gov/cgi/cbook.cgi?ID=C7440508&Units=SI&Mask=2#Thermo-Condensed> (Cu)

7. RESPONSIBILITY NOTICE

The authors are the only responsible for the printed material included in this paper.